Proceedings of the 20th International Conference on Soil Mechanics and Geotechnical Engineering– Rahman and Jaksa (Eds)

Discrete element simulation of the response of a double-twisted mesh subject to cyclic loads

Simulation par éléments discrets de la réponse d'un maillage double torsion soumis à des charges cycliques

Marco Previtali, **Matteo Ciantia**, Saverio Spadea
School of Science and Engineering, University of Dundee, United Kingdom, m.o.ciantia@dundee.ac.uk,

Riccardo Castellanza, Giovanni Crosta
Department of Earth and Environmental Sciences, University of Milano-Bicocca, Italy

ABSTRACT: Flexible protection barriers are the most widespread passive mitigation system against natural hazards such as rockfall. These structures dissipate the kinetic energy of the rock block through inertial deformation. When subject to significant loads, the steel wires composing the structure undergo plastic hardening and non-reversible deformation. While this phenomenon is well known, and the literature contains studies of the mesh plasticization phenomenon, the non-reversibility of this process is not considered for the successive impact events. Herein a Discrete Element model is employed to investigate the cyclic response of a double-twisted hexagonal wire mesh during a quasi-static punch test. The results show that repeated low entity loads, 12% of the peak force, only cause negligible plasticization within the mesh; medium loads, 60% of the peak force, can induce sagging and changes in the post-peak response, without significantly affecting the peak load. Finally, high loads, 80% of the peak force, quickly induce failure within the mesh.

RÉSUMÉ : Les barrières de protection flexibles sont le système d'atténuation passive le plus répandu contre les risques naturels tels que les chutes de pierres. Ces structures dissipent l'énergie cinétique du bloc rocheux par déformation inertielle. Soumis à des charges importantes, les fils d'acier composant la structure subissent un durcissement plastique et une déformation irréversible. Bien que ce phénomène soit bien connu et que la littérature contienne des études sur le phénomène de plastification du maillage, cela n'est généralement pas pris en compte pour les événements d'impact successifs. Dans cet article, un modèle d'élément discret est utilisé pour étudier la réponse cyclique d'un treillis métallique hexagonal à double torsion lors d'un test de poinçonnage quasi-statique. Les résultats montrent que les faibles charges d'entité répétées, 12% de la force maximale, ne provoquent qu'une plastification négligeable dans le maillage ; des charges moyennes, 60% de la force de pointe, peuvent induire un affaissement et des changements dans la réponse post-crête, sans affecter de manière significative la charge de pointe. Enfin, des charges élevées, 80% de la force maximale, induisent rapidement une rupture au sein du maillage.

KEYWORDS: Discrete Element Method, Cyclic loading, Flexible protection structure, double-twisted mesh, Plasticization

1 INTRODUCTION

Rockfall is a natural hazard posing a threat to human life and infrastructure. Flexible protection systems, steel wire meshes that catch the block during its movement, are one of the more commonly employed mitigation procedures. By using a combination of onset probability (Jaboyedoff et al., 2001; Valagussa et al., 2014) and block propagation analysis (Crosta et al., 2005; Bourrier et al., 2014), a quantitative characterization of both the expected impact energy and frequency on a given barrier is now possible and can be used to guide the design phase.

With the advancement of computational power, numerical techniques such as the Finite Element Method (FEM) (Govoni et al., 2011; Gentilini et al., 2012; Castanon-Jano et al., 2018) and the Discrete Element Method (DEM) (Bertrand et al., 2005; Thoeni et al., 2013; Pol et al., 2021) have become common tools to investigate the behaviour of these barriers. As these models need to account for contact interactions, large deformations, and dynamic effects, which typically require explicit time integration schemes, efficiency can be an issue. This is typically mitigated using a multi-scale approach, in which the small-scale barrier components are not modelled explicitly but they are instead substituted at the meso-scale by numerical objects that replicate their behaviour. For example, a piece of wire is substituted by a thin beam characterized by the same force-displacement curve. Material plasticity is implemented using bilinear (Foti and de Luca di Roseto, 2016; Cui et al., 2018; Zhao et al., 2020) and multi-linear (Thoeni et al., 2013; Mentani et al., 2016) force-displacement curves. While these plasticity models have been used to investigate the mesh behaviour during the impact loads (Mentani et al., 2016; Previtali et al., 2021), it is difficult to find examples of cyclic barrier response in the literature.

In this study, the cyclic response of a double-twisted hexagonal mesh is investigated through numerical quasi-static punch tests, to quantify the variation in the barrier bearing capacity after repeated loads. Double-twisted hexagonal meshes have been chosen as they are one of the most widespread designs. Additionally, they are characterized by higher degrees of plasticization than other low energy mesh designs (i.e. diamond-shaped (Buzzi and Krummenacher, 2014).

2 MODEL SETUP

2.1 *Numerical model*

The DEM is used to simulate the movement of a large number of discrete particles, characterized by mass, shape and volume, following Newton's laws of motion. In the soft-sphere DEM formulation, contact interactions are solved by allowing these particles to overlap with each other during the simulation (O'Sullivan, 2011). When two particles overlap, a contact is generated and a repulsive force is applied to two particles at the ends of the contact, considering the overlap distance as the

compression of an elastic spring (Hooke's Law). By extending the contact interactions to tension, i.e. generating a bond between the particles, it is possible to model the behaviour of cemented materials (Potyondy and Cundall, 2004) and, by increasing the reference inter-particle distance, to simulate the behaviour of beams and trusses (Brown *et al.*, 2014; Previtali *et al.*, 2020b). In this paper, the mesh wires are represented using a set of discrete particles connected by remote interactions (Potyondy and Cundall, 2004), that replicate the known elasto-plastic wire behaviour through experimental multilinear force-displacement curves for single-wire (SW) and double-twist (DT) interactions (Thoeni et al., 2013). This wire-based approach, as defined by (Pol et al., 2021), is characterized by high efficiency due to the low number of DEM elements employed, while maintaining a high grade of accuracy when the mesh is in contact with objects larger than the maximum distance between its elements (Pol *et al.*, 2017). Figure 1 shows the remote interaction contact law used to describe the tensile behaviour of both SW and DT mesh elements (Thoeni et al., 2013). The figure also graphically represents both the elastic and plastic energy repartitions that will be used to interpret the numerical results. These are defined as:

$$E_P = \int_0^l f(\Delta l)dl - E_E \tag{1}$$

$$E_E = 0.5 E s_a \Delta l \tag{2}$$

where l is the wire length, E is the material Young Modulus, f is the force-displacement curve, s_a is the wire section area and Δl is the change in wire length (positive in tension).

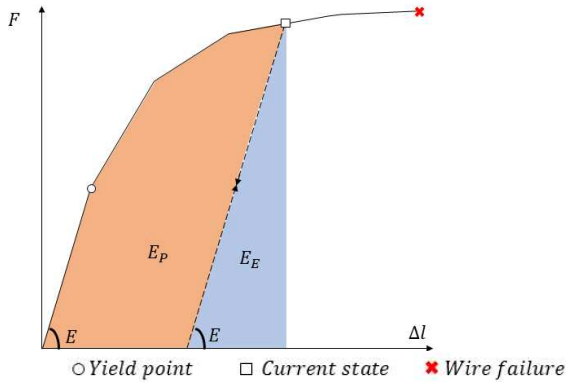

Figure 1: Elastic-plastic contact model for DT and SW wires

For additional details on the energy repartition refer to Previtali *et al.*, (2021). A viscous damping value of 0.5 is applied to the wire contacts, following (Thoeni *et al.*, 2013). While this value is relatively large, it was found to have no influence on the system response under quasi-static conditions (Thoeni *et al.*, 2013) and is therefore used to reduce the low-energy oscillations within the mesh. Wire failure is taken into account by deleting the contact once its plastic strain becomes higher than the experimental threshold (Thoeni et al., 2013). The platter-mesh and boulder-mesh interactions are carried out with a linear elastic contact model. All the numerical parameters are listed in Table 1. The model was calibrated on experimental literature data (Bertrand *et al.*, 2008) using quasi-static tensile and punch tests, following (Pol *et al.*, 2017). For further details, refer to (Previtali *et al.*, 2020b). While no experimental data is available at the current time to verify the quasi-static cyclic response, the plastic hardening constitutive model was shown to reproduce the macroscopic unloading behaviour under dynamic conditions (Thoeni *et al.*, 2013).

The wire geometries are discretized using 2 DEM elements each, following Previtali *et al.*, (2020a), as their bending stiffness is considered negligible (Thoeni et al., 2013). To obtain the real mesh mass, the particle radius is set to 5.4 mm and its density to 6500 kg/m^3. The simulations presented herein are carried out with the DEM code PFC3D (Itasca Consulting Group, 2014).

Table 1: DEM model contact parameters

Parameter	*Symbol*	Value
Single Wire Young Modulus [10^8 Pa]	E_{sw}	200.0
Double-Twist Young Modulus [10^8 Pa]	E_{dt}	100.0
Single Wire section area [mm^2]	$s_{a,sw}$	7.0
Double-Twist section area [mm^2]	$s_{a,dt}$	14.0
Single Wire Yield Stress [10^8 Pa]	y_{sw}	3.02
Double-Twist Yield Stress [10^8 Pa]	y_{dt}	2.0
Single Wire plastic strain at failure [-]	$\varepsilon_{pf,sw}$	0.19
Double-Twist plastic strain at failure [-]	$\varepsilon_{pf,dt}$	0.17
Numerical damping [-]	β	0.5
Wall contact stiffness [10^8 N/m]	k_n	0.0
Normal / shear stiffness ratio [-]	k_{ratio}	10.0
Wall contact friction [-]	μ	0.2

2.2 *Test setup*

Following Bertrand et al., (2008) the double-twisted mesh is modelled by a repeating hexagonal pattern, with major and minor length of 0.1 and 0.08 meters, formed by the interweavement of two 3 millimetres thick wires.

The mesh panel, formed by a 3x3 meters square of interweaved hexagonal mesh, is loaded by a truncated spheroid platter with radius of 0.5 m and height of 15 cm (Figure 2) (Bertrand *et al.*, 2008; UNI11437, 2012; Previtali *et al.*, 2020b). The initial test conditions are obtained by placing a horizontal wall 0.1 meters beneath the base of the mesh and letting the barrier deform under its own weight.

A preliminary test is carried out through a displacement-controlled platter, in order to identify the force and displacement at which the mesh fails under monotonic loads. Successively, three cyclic load tests are carried out through a force-controlled servo with a maximum speed of 0.02 m/s. The target forces (F^*) employed are 3, 15 and 20 kN, respectively 12%, 60% and 80% of the force recorded at failure during the monotonic loading test (25 kN). Table 2 lists all the test parameters. Finally, a second monotonic load test is carried out to the pre-plasticized mesh. For this test, the final state of the 15 kN cyclic test is employed. The platter is brought back to a zero-force condition before applying the constant displacement rate.

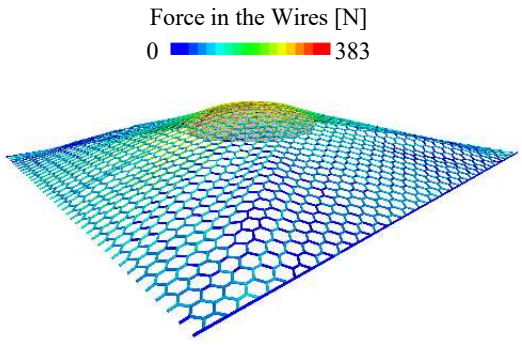

Figure 2: Quasi-static mesh punch test.

Table 2: Cyclic load tests parameters and results

Test number	1	2	3
Force [kN]	3	15	20
Number of cycles [$-$]	12	6	4
Plastic energy dissipated [kN]	<1e-2	0.63	1.9

3. RESULTS

3.1 Monotonic displacement test

During the preliminary test (Figure 3,4), the force acting on the platter increases slowly as the mesh is displaced without causing any tensile deformation of the mesh elements. In this phase the platter load corresponds to the weight of the mesh. When the platter displacement (u_P) reaches 20 cm, point (a), the mesh starts loading and the force on the platter increases exponentially (Bertrand et al., 2008; Pol et al., 2017; Previtali et al., 2020b). The tensile forces within the mesh assume a cross-like pattern (Mentani et al., 2018), which progressively transform in a cross-like shape (point b, c). At $u_P = 0.42$ m, most of the wires reach the yield point and the energy dissipated through plastic deformation increases linearly with the platter displacement. Before mesh failure occurs, the SW contacts exhibit higher plasticization than the DT contacts (Figure 5a). The area affected by plasticization is mostly limited to the platter contact area for the single wires, while for the DT it is oriented in the direction of maximum tension, parallel to the DT interweavements due to their higher stiffness. The peak contact force, 25kN, occurs at $u_P = 0.53$ m, (point c) as the wires in contact with the platter reach the plastic strain threshold (point c). In the final portion of the simulation (point d, e, f) the force on the platter increases in-between failure events: the mesh develops a cut driven by the maximum tension, parallel to the DT, and the minimum resistance, the SW. As the failure path propagates to the bottom of the mesh, Figure f, it changes direction in order to satisfy the criteria of minimum resistance.

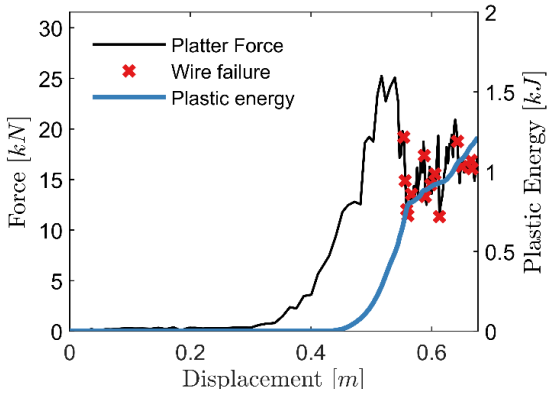

Figure 3: Force-Displacement curve of the platter during the monotonic displacement punch test.

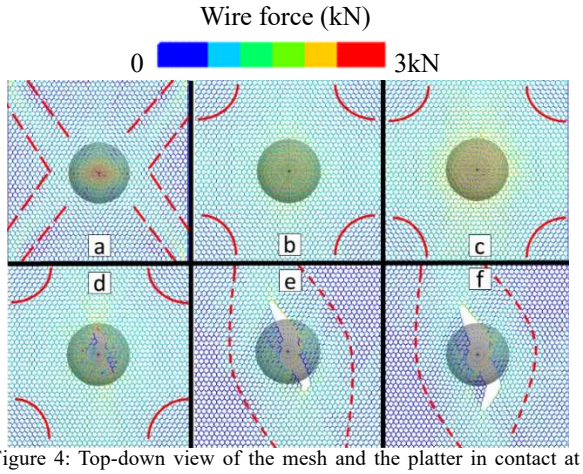

Figure 4: Top-down view of the mesh and the platter in contact at different time instants.

(a)

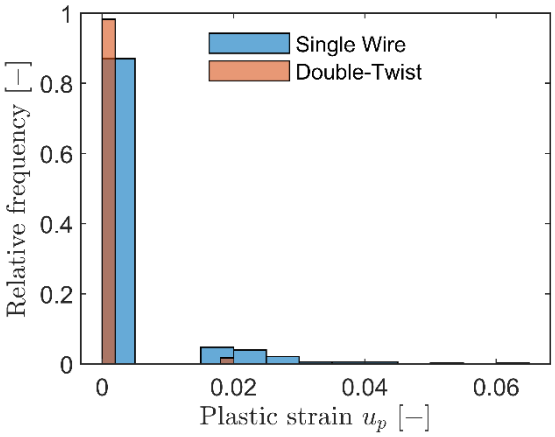

(b)

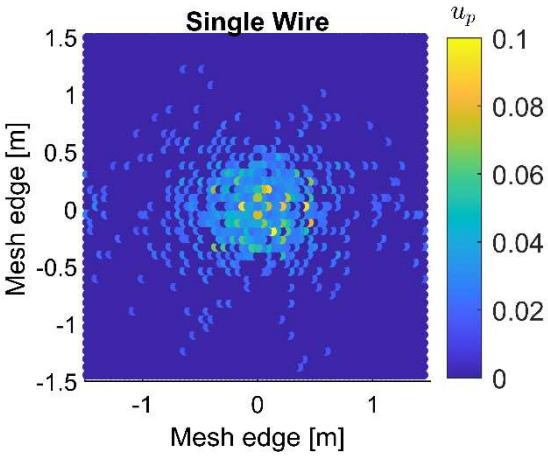

(c)

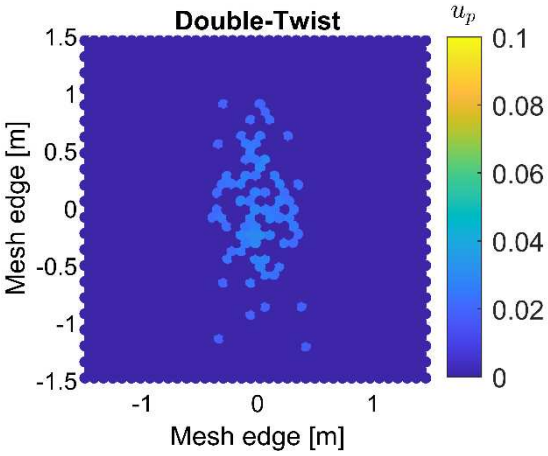

Figure 5 Monotonic load test: a) Relative frequency histograms of the plastic strain within the wires, maps of the plastic strains within (b) the single wires, (c) the double-twists.

3.2 Cyclic load tests

During Test #1, the minimum and maximum barrier displacement do not change during the test as negligible mesh plasticization is achieved (Figure 6a). In Test #2, plastic energy increment of 0.55 kN is attained during the first cycle, which progressively decreases, becoming negligible from the 4th cycle (Figure 6b). Most of the plasticization occurs within the first cycle, as the plastic energy only increases by 0.5 kJ (from 0.36 to 0.41) during the cyclic portion of the test. Finally, during Test #3, the same amount of energy is dissipated in cycle 2 and 3 (0.4 kN). The platter displacement at $F = 0\ kN$ (i.e. unloading) and $F = F^*$ (i.e. peak load) also increases with cycles as the wires plasticize. A portion of the wires fails during the 3rd cycle, while mesh failure occurs during the 4th cycle.

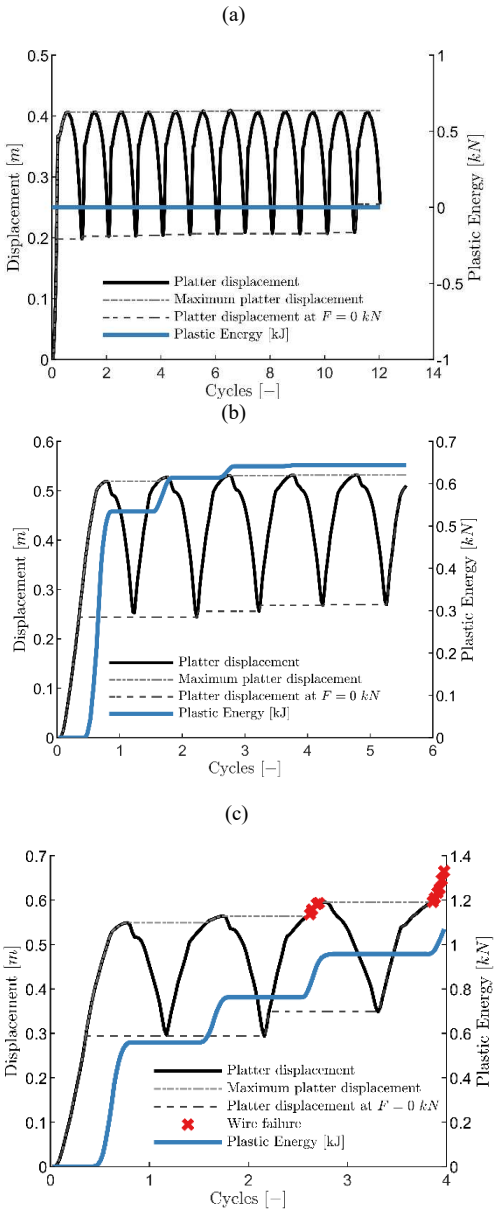

Figure 6: Platter displacement during the (a) Test #1, (b) Test #2 and (c) Test #3.

3.3 Monotonic load on pre-plasticized mesh

During the test, the force-displacement curve of the platter is similar to the one of the first monotonic displacement test, reaching a peak force value of 24.5 kN. The main difference is the initial and final plastic energy within the mesh, which differs due to mesh pre-plasticization (Figure 5 vs Figure 8b). The fact that the double-twist interactions also present plasticity before the maximum load (Figure 8a) causes them to fail during post-peak, which does not occur during the direct loading.

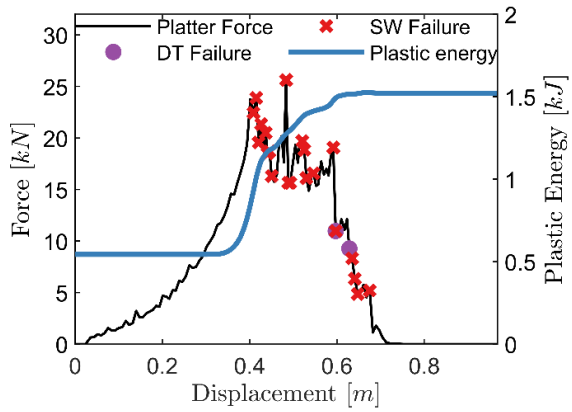

Figure 7: Force-displacement curve for the monotonic load on the pre-plasticized mesh.

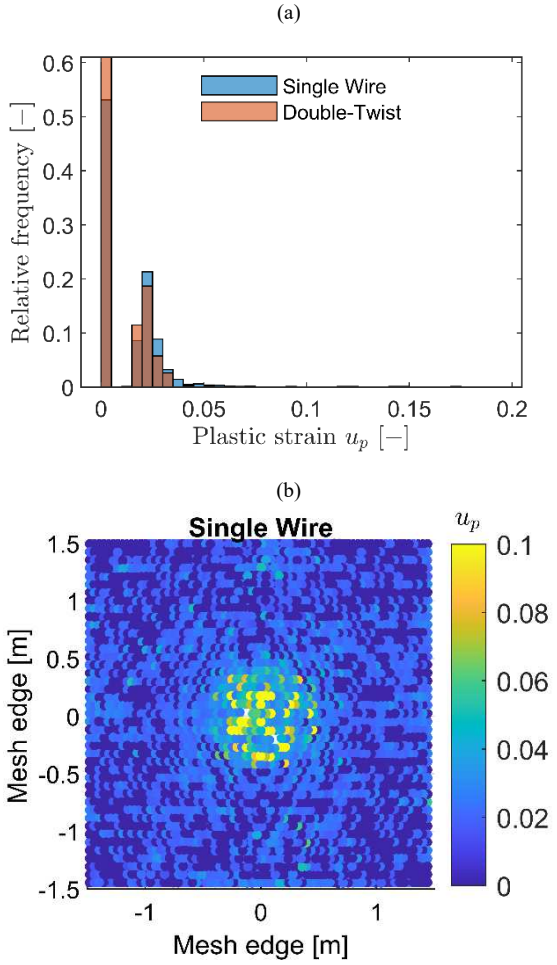

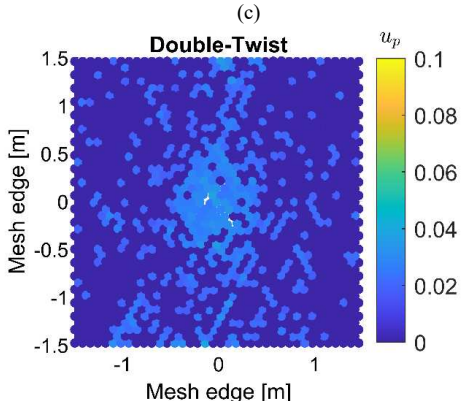

Figure 8: Monotonic load test on the pre-plasticized mesh: a) Relative frequency histograms of the plastic strain within the wires, maps of the plastic strains within (b) the single wires, (c) the double-twists.

4 CONCLUSIONS

A numerical model of a double-twisted wire mesh, based on the remote contact DEM approach is employed to investigate the mesh response to cyclic loads. Two displacement controlled and three force-controlled cyclic tests have been carried out. The low energy cyclic test (3kN) shows that the mesh is unaffected by cyclic impacts of low entity. A cyclic force equal to 60% of the peak induces significant plasticization in the mesh but it is however insufficient to induce failure on its own as the plastic energy increments become negligible after a few cycles. Although this can cause structural problems within the mesh (i.e. excessive sagging), it does not significantly increment the risk of wire failure when the mesh is again loaded until failure (4% decrease in peak force). On the other hand, this can pose a problem for the mesh resilience under post-failure conditions: the higher overall plasticization causes the double-twist contacts to fail as well, allowing the laceration in the mesh to propagate in other directions, widening the potential hole. Finally, the cyclic loading at 80% of the peak strength quickly produces material failure, during the 3rd cycle. The tests also highlight the inadequacy of total mesh plasticization as an indicator of mesh deterioration, as the various plasticization patterns that can develop within the mesh under the differed loading conditions have a greater influence in lowering the peak strength of the mesh compared to the absolute value. For future studies, it would be useful to investigate how these patterns affect the post-peak response and to carry out more cyclic tests in order to pinpoint the force threshold at which the mesh undergoes failure under repeated loading.

5 REFERENCES

Bertrand, D., Nicot, F., Gotteland, P. and Lambert, S. (2005) Modelling a geo-composite cell using discrete analysis, *Computers and Geotechnics*, 32(8), pp. 564–577. doi: 10.1016/j.compgeo.2005.11.004.

Bertrand, D., Nicot, F., Gotteland, P. and Lambert, S. (2008) Discrete element method (DEM) numerical modeling of double-twisted hexagonal mesh, *Canadian Geotechnical Journal*, 45(8), pp. 1104–1117. doi: 10.1139/T08-036.

Bourrier, F., Lambert, S. and Baroth, J. (2014) A Reliability-Based Approach for the Design of Rockfall Protection Fences, *Rock Mechanics and Rock Engineering.* Springer-Verlag Wien, 48(1), pp. 247–259. doi: 10.1007/s00603-013-0540-2.

Brown, N. J., Chen, J. F. and Ooi, J. Y. (2014) A bond model for DEM simulation of cementitious materials and deformable structures, *Granular Matter*. Springer New York LLC, 16(3), pp. 299–311. doi: 10.1007/s10035-014-0494-4.

Buzzi, O. and Krummenacher, E. L. B. (2014) Performance of High Strength Rock Fall Meshes : Effect of Block Size and Mesh Geometry. doi: 10.1007/s00603-014-0640-7.

Castanon-Jano, L., Blanco-Fernandez, E., Castro-Fresno, D. and Ferreño, D. (2018) Use of explicit FEM models for the structural and parametrical analysis of rockfall protection barriers, *Engineering Structures.* Elsevier Ltd, 166, pp. 212–226. doi: 10.1016/j.engstruct.2018.03.064.

Crosta, G., Agliardi, F. and Frattini, P. (2005) Modelling rockfall impact on structures. DE, 7, pp. 8555–8555.

Cui, L., Wang, M. and Yu, T. (2018) Dynamic Finite Element Analysis of a New Type Flexible Rock Shed under the Impact of Rock Block and Improving the Design, Shock and Vibration. Hindawi Limited, 2018. doi: 10.1155/2018/1936560.

Foti, F. and de Luca di Roseto, A. (2016) Analytical and finite element modelling of the elastic–plastic behaviour of metallic strands under axial–torsional loads, *International Journal of Mechanical Sciences.* Elsevier Ltd, 115–116, pp. 202–214. doi: 10.1016/j.ijmecsci.2016.06.016.

Gentilini, C., Govoni, L., de Miranda, S., Gottardi, G. and Ubertini, F. (2012) Three-dimensional numerical modelling of falling rock protection barriers, *Computers and Geotechnics.* Elsevier, 44, pp. 58–72. doi: 10.1016/J.COMPGEO.2012.03.011.

Govoni, L., de Miranda, S., Gentilini, C., Gottardi, G. and Ubertini, F. (2011) Modelling of falling rock protection barriers, *International Journal of Physical Modelling in Geotechnics.* Thomas Telford Services Ltd, 11(4), pp. 126–137. doi: 10.1680/ijpmg.2011.11.4.126.

Itasca Consulting Group (2014) PFC (particle flow code in 2 and 3 dimensions), version 5.0 [User's manual].

Jaboyedoff, M., Baillifard, F., Hantz, D., Heidenreich, B. and Bazzoccola, D. (2001) Prévention des mouvements de versant et des instabilités de falaises. Confrontation des méthodes d'étude des éboulements rocheux dans l'arc alpin. doi: 10.13140/2.1.1285.2801.

Mentani, A., Giacomini, A., Buzzi, O., Govoni, L., Gottardi, G. and Fityus, S. (2016) Numerical Modelling of a Low-Energy Rockfall Barrier: New Insight into the Bullet Effect, *Rock Mechanics and Rock Engineering.* Springer Vienna, 49(4), pp. 1247–1262. doi: 10.1007/s00603-015-0803-1.

Mentani, A., Govoni, L., Giacomini, A., Gottardi, G. and Buzzi, O. (2018) An Equivalent Continuum Approach to Efficiently Model the Response of Steel Wire Meshes to Rockfall Impacts, *Rock Mechanics and Rock Engineering.* Springer-Verlag Wien, 51(9), pp. 2825–2838. doi: 10.1007/s00603-018-1490-5.

O'Sullivan, C. (2011) Particulate discrete element modelling: a geomechanics perspective. CRC Press.

Pol, A., Gabrieli, F. and Brezzi, L. (2021) Discrete element analysis of the punching behaviour of a secured drapery system: from laboratory characterization to idealized in situ conditions, *Acta Geotechnica.* Springer Science and Business Media Deutschland GmbH, pp. 1–21. doi: 10.1007/s11440-020-01119-z.

Pol, A., Thoeni, K. and Mazzon, N. (2017) Discrete Element Modelling of punch tests with a double-twist hexagonal wire mesh.

Potyondy, D. O. and Cundall, P. A. (2004) A bonded-particle model for rock, *International Journal of Rock Mechanics and Mining Sciences*, 41(8), pp. 1329–1364. doi: 10.1016/j.ijrmms.2004.09.011.

Previtali, M., Ciantia, M., Castellanza, R. and Crosta, G. B. (2020a) Mesh sensitivity in discrete element simulation of flexible protection structures. Loughborough University. doi: 10.17028/rd.lboro.12102534.v1.

Previtali, M., Ciantia, M. O., Spadea, S., Castellanza, R. and Crosta, G. B. (2021) Multiscale modelling of dynamic impact on highly deformable compound rockfall fence nets, *Proceedings of the Institution of Civil Engineers - Geotechnical Engineering*.

Previtali, M., Ciantia, M., Spadea, S., Castellanza, R. and Crosta, G. (2020b) Discrete element modeling of compound rockfall fence nets, in IACMAG2020, pp. 1–8.

Thoeni, K., Lambert, C., Giacomini, A. and Sloan, S. W. (2013) Discrete modelling of hexagonal wire meshes with a stochastically distorted contact model, *Computers and Geotechnics.* Elsevier, 49, pp. 158–169. doi: 10.1016/J.COMPGEO.2012.10.014.

UNI11437 (2012) UNI 11437:Rockfall protective measures - Test on meshes for slopes coverage. Italy.

Valagussa, A., Frattini, P. and Crosta, G. B. (2014) Earthquake-induced rockfall hazard zoning, Engineering Geology. Elsevier, 182, pp. 213–225. doi: 10.1016/J.ENGGEO.2014.07.009.

Zhao, L., Yu, Z. X., Liu, Y. P., He, J. W., Chan, S. L. and Zhao, S. C. (2020) Numerical simulation of responses of flexible rockfall barriers under impact loading at different positions, *Journal of Constructional Steel Research.* Elsevier Ltd, 167, p. 105953. doi: 10.1016/j.jcsr.2020.105953.